Optimal Design of WAIMs over Patch Arrays for 5G Applications

G. Oliveri, A. Polo, M. Salucci, G. Gottardi, and A. Massa

Contents

1 SbD Synthesis Tool: implementation and validation

To implement the SbD Synthesis Tool, we used a Particle Swarm Optimizer (PSO). This optimization technique allows to define a swarm of particles that will explore the solution space in order to find the optimal solution. The software is been implemented in order to be able to handle the optimization of single or multiple WAIM layers, composed by both isotropic or anisotropic materials.

1.1 $\varepsilon^{sub} = 12.8$ Tests

1.1.1 Test Case #1 - Single Frequency - 1 Isotropic WAIM Layer - $\varepsilon^1 = [1 : 5] + j0$ - Square Lattice - $\varepsilon^{sub} = 12.8$ Tests

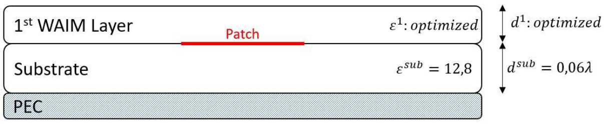

Figure 1: Test Case Schema.

Simulation Parameters:

- Frequency: $f = 10[GHz]$;
- Patch dimensions: $w = 0.15$, $l = 0.098$ $[\lambda]$;
- Probe position: $x = 0.049$, $y = 0.0$ $[\lambda]$;
- Substrate: $\varepsilon_x = 12.8 + j0$, $\varepsilon_y = 12.8 + j0$, $\varepsilon_z = 12.8 + j0$, $d = 0.06[\lambda]$
- Floquet coefficient $= 121$;
- Lattice basis: $s_1 = (0.5, 0.0)$, $s_2 = (0.0, 0.5)$ $[\lambda]$;

Analysis Parameters:

- Samples analysis (phi cuts): $\theta \in [0, 90]$ $[deg]$, $\varphi \in [0, 90]$ $[deg]$, $\theta_{samples} = 182$, $\varphi_{samples} = 3$;
- Samples analysis (3D plots): $\theta \in [-180, 180]$ $[deg]$, $\varphi \in [-90, 90]$ $[deg]$, $\theta_{samples} = 72$, $\varphi_{samples} = 21$;

PSO Synthesis Parameters:

- Number of WAIM Layers: $N = 1$;
- Unknowns: $U = 2$;
- Unknown ranges: $\varepsilon = [1 : 5] + j0$, $d = [0.033 : 0.5]$ $[\lambda]$;
- Swarm size: $P = 6$;

- Max iteration number: $I = 80$;
- Inertial weight$= 0.4$;
- Alpha$= 0.4$;
- Beta$= 0.4$;
- C1$= 2.0$;
- C2$= 2.0$;
- Random seed$= 26$;
- No-WAIM case implemented by the first particle at the 1^{st} iteration;
- Samples synthesis (phi cuts): $\theta \in [0,\, 90]\,[deg]$, $\varphi \in [0,\, 90]\,[deg]$, $\theta_{samples} = 7$, $\varphi_{samples} = 3$;

Optimization Results

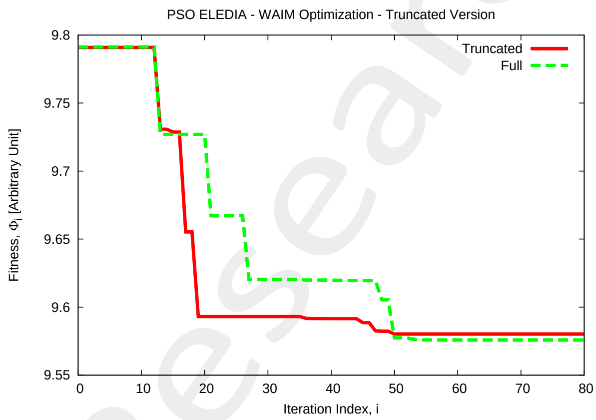

Figure 2: Fitness Dynamics.

$$Simulation\,time\,(Truncated):\; 298m\,42s$$

$$Simulation\,time\,(Full):\; 1132m\,38s$$

We ran the optimization using both the full and the truncated version of the software, with the same parameters, in order to identify some possible differences, but the simulations ended up with almost the same results.

$Tool$	$Optimal\,Solution$		$Fitness\,Value$	
	$\varepsilon_x^1 = \varepsilon_y^1 = \varepsilon_z^1$	$h^1\,[\lambda]$	$\Phi_{i=0}$	$\Phi_{I=80}$
$Truncated$	1.0154	0.5	9.791	9.580
$Full$	1.0153	0.5	9.791	9.576

Table 1: Optimal Solutions.

Even if the "Full" simulation has a lower Fitness value, the difference with respect to the "Truncated" case is very tiny, compared with the difference in computational time. Therefore, for the next simulations we will run only the "Truncated" version.

This first simulation takes as example the one performed, but considers different ranges. In particular, the most important difference is on the ε^1 range: is set as $[-5 : 5]$. This allowed to explore solution with ε^1 lower than 1 (Free Space), and even negative solutions.

Our case, instead, takes as borderline case the Free Space solution ($\varepsilon^1 = [1 : 5]$). Indeed, as reported in the previous table (Table 1 on page 4), we can notice that the optimal solution has a value of ε^1 very close to 1.

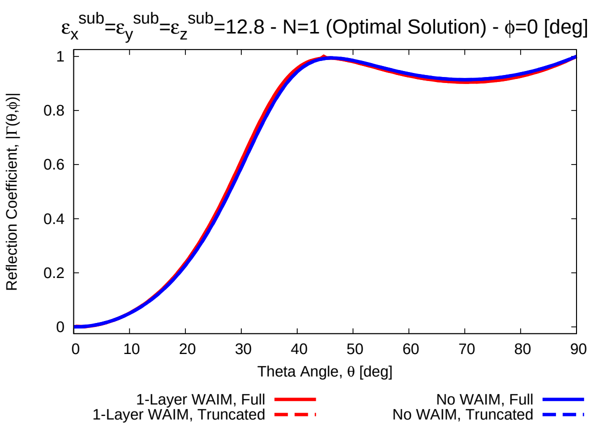

$(a)\ \varphi = 0[deg]$

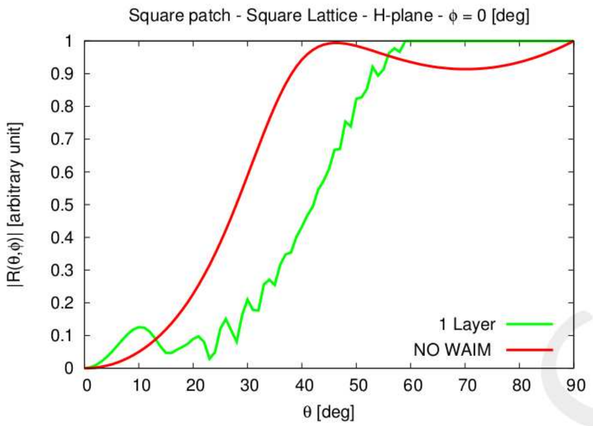

$(b)\ \varphi = 0[deg]$, from reference report

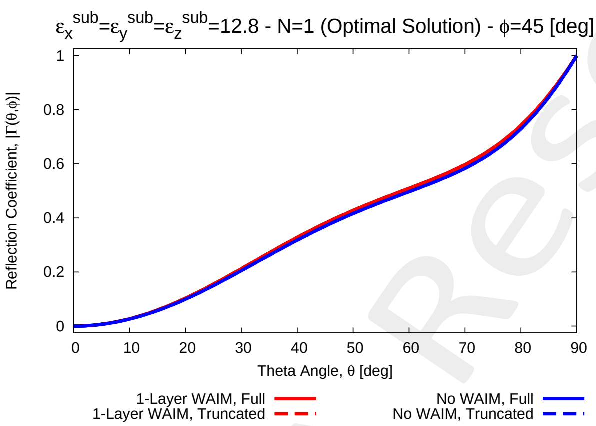

$(c)\ \varphi = 45[deg]$

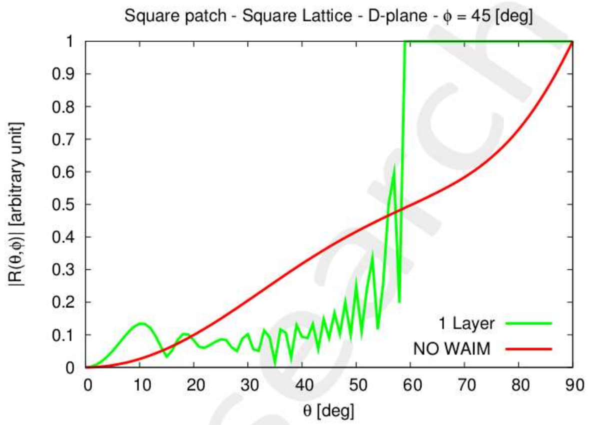

$(d)\ \varphi = 45[deg]$, from reference report

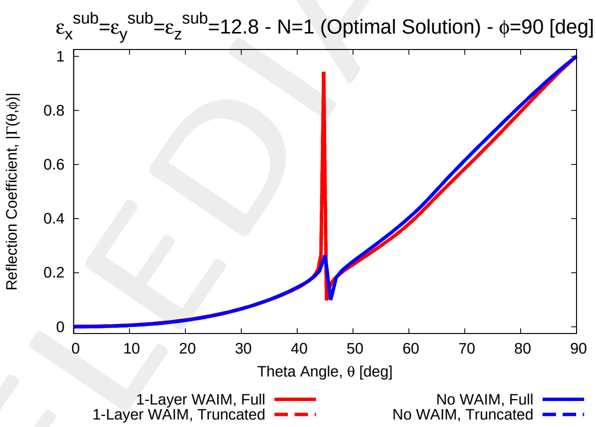

$(e)\ \varphi = 90[deg]$

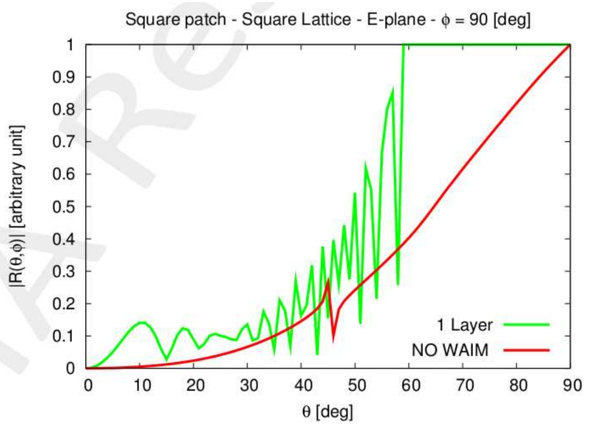

$(f)\ \varphi = 90[deg]$, from reference report

Figure 3: Reflection Coefficient along φ cuts, 1 Layer WAIM.

The higher peak in Figure 3 on page 5(e) is probably due to a more dense sampling along θ.

From the images, we can notice that our solution is almost identical to the non-covered case, but it slightly reduces the Reflection Coefficient $\Gamma$for values of $\theta > 80[deg]$. On the contrary, the solution proposed has an high non linear behaviour and a total reflection for $\theta > 60[deg]$.

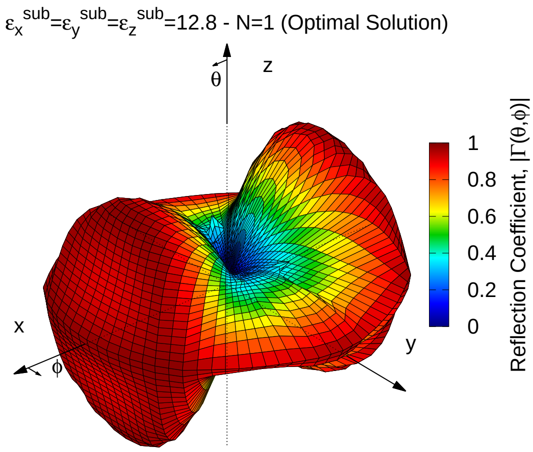

(a) Γ, 1 Layer WAIM, "Full"

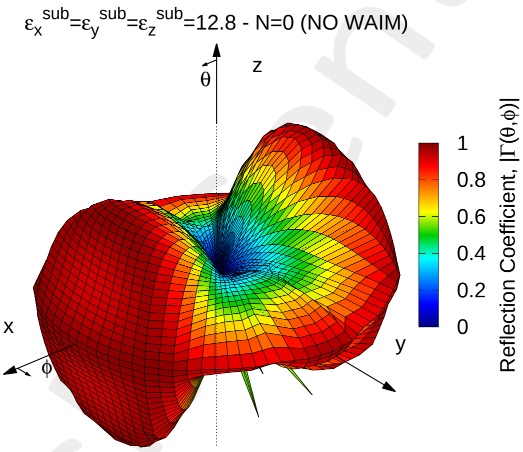

(b) Γ, No-WAIM

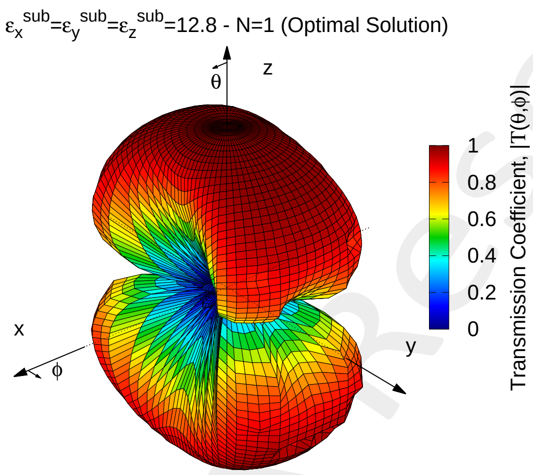

(c) $|T|^2$, 1 Layer WAIM, "Full"

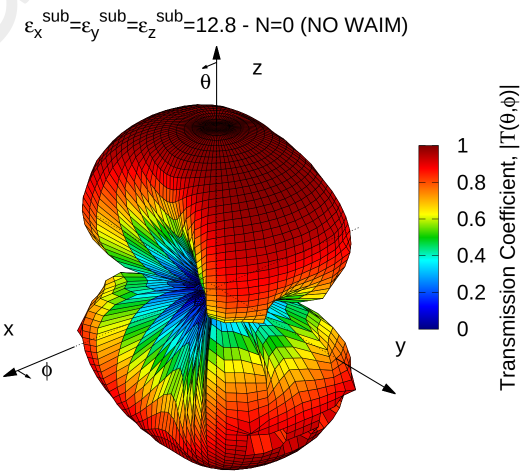

(d) $|T|^2$, No-WAIM

Figure 4: Reflection Coefficient and Transmission Coefficient

Tool	*Cost Function*		*Improvement Percentage*
	Φ_0^{fine}	Φ_{SbD}^{fine}	
Full	663.46	661.75	-0.26%
Truncated	663.51	661.72	-0.27%

Table 2: Cost Function Improvement.

1.1.2 Test Case #2 - Single Frequency - 1 Isotropic WAIM Layer - $\varepsilon^1 = [1 : 35] + j0$ - Square Lattice - $\varepsilon^{sub} = 12.8$ Tests

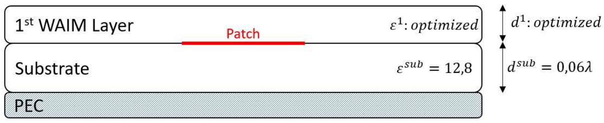

Figure 5: Test Case Schema.

Simulation Parameters:

- Frequency: $f = 10[GHz]$;
- Patch dimensions: $w = 0.15$, $l = 0.098$ $[\lambda]$;
- Probe position: $x = 0.049$, $y = 0.0$ $[\lambda]$;
- Substrate: $\varepsilon_x = 12.8 + j0$, $\varepsilon_y = 12.8 + j0$, $\varepsilon_z = 12.8 + j0$, $d = 0.06[\lambda]$
- Floquet coefficient $= 121$;
- Lattice basis: $s_1 = (0.5, 0.0)$, $s_2 = (0.0, 0.5)$ $[\lambda]$;

Analysis Parameters:

- Samples analysis (phi cuts): $\theta \in [0, 90]$ $[deg]$, $\varphi \in [0, 90]$ $[deg]$, $\theta_{samples} = 182$, $\varphi_{samples} = 3$;
- Samples analysis (3D plots): $\theta \in [-180, 180]$ $[deg]$, $\varphi \in [-90, 90]$ $[deg]$, $\theta_{samples} = 72$, $\varphi_{samples} = 21$;

PSO Synthesis Parameters:

- Number of WAIM Layers: $N = 1$;
- Unknowns: $U = 2$;
- Unknown ranges: $\varepsilon = [1 : 35] + j0$, $d = [0.033 : 0.5]$ $[\lambda]$;
- Swarm size: $P = 6$;
- Max iteration number: $I = 80$;
- Inertial weight$= 0.4$;
- Alpha$= 0.4$;
- Beta$= 0.4$;
- C1$= 2.0$;
- C2$= 2.0$;

- Random seed$=26$;
- No-WAIM case implemented by the first particle at the 1^{st} iteration;
- Samples synthesis (phi cuts): $\theta \in [0,\,90]\,[deg]$, $\varphi \in [0,\,90]\,[deg]$, $\theta_{samples} = 7$, $\varphi_{samples} = 3$;

Optimization Results

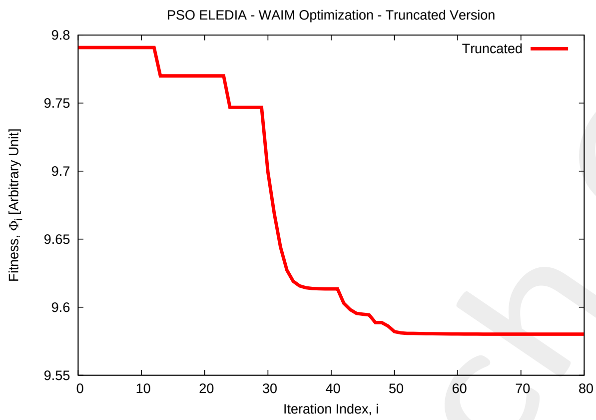

Figure 6: Fitness Dynamics.

$$Simulation\,time\,(Truncated):\;299m\,01s$$

Since the results obtained in 1.1.1 are very similar to the ones obtained for the Non-Covered case, in this simulation we enlarged the solution space by setting $\varepsilon^1 = [1\,:\,35]$.

$Tool$	$Optimal\,Solution$		$Fitness\,Value$	
	$\varepsilon_x^1 = \varepsilon_y^1 = \varepsilon_z^1$	$h^1\,[\lambda]$	$\Phi_{i=0}$	$\Phi_{I=80}$
$Truncated$	1.015	0.5	9.791	9.580

Table 3: Optimal Solution.

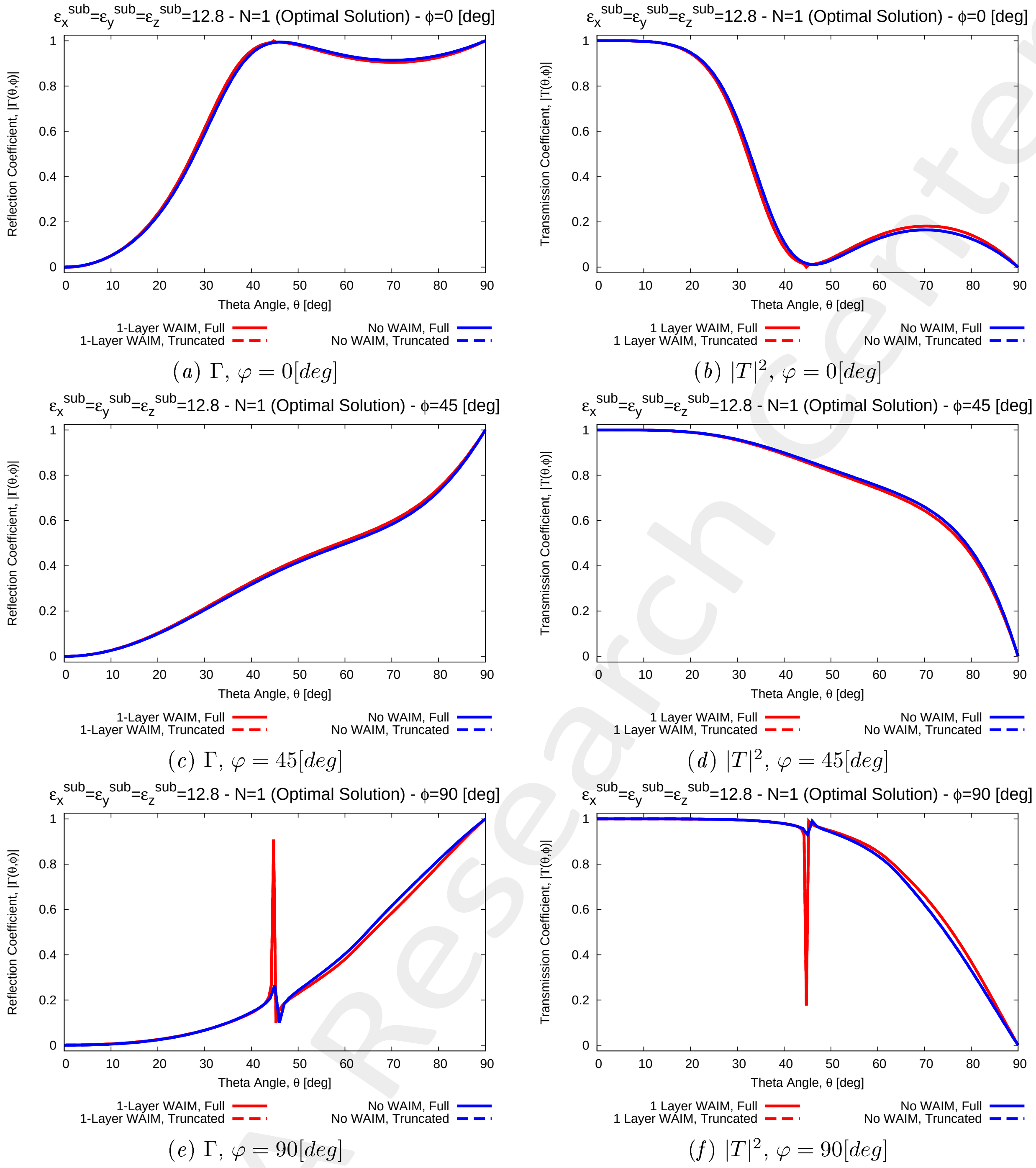

$(a)\ \Gamma,\ \varphi = 0[deg]$ $(b)\ |T|^2,\ \varphi = 0[deg]$

$(c)\ \Gamma,\ \varphi = 45[deg]$ $(d)\ |T|^2,\ \varphi = 45[deg]$

$(e)\ \Gamma,\ \varphi = 90[deg]$ $(f)\ |T|^2,\ \varphi = 90[deg]$

Figure 7: Reflection Coefficient along φ cuts, 1 Layer WAIM.

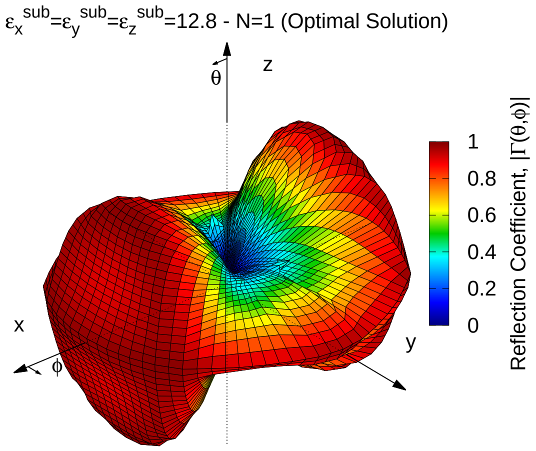

(a) Γ, 1 Layer WAIM, "Full"

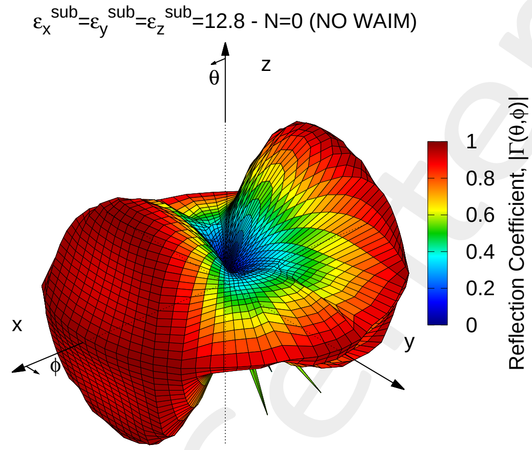

(b) Γ, No-WAIM

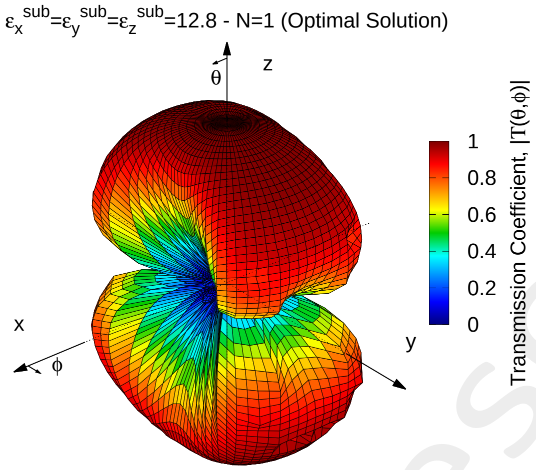

(c) $|T|^2$, 1 Layer WAIM, "Full"

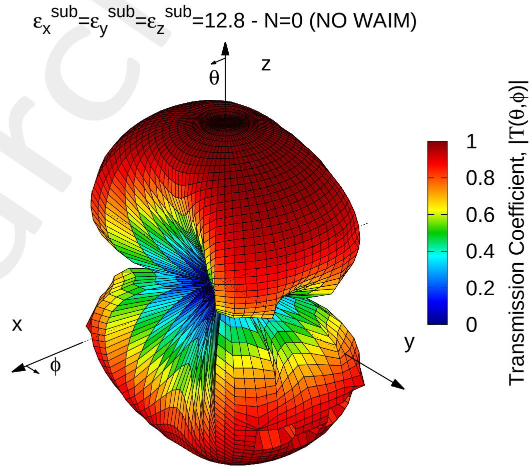

(d) $|T|^2$, No-WAIM

Figure 8: Reflection Coefficient and Transmission Coefficient

As we can notice, the obtained value are still very close to the No-WAIM case. Moreover, increasing the maximum value of ε^1 has not lead to any improvement, since the optimal solution still tends to the Free Space.

Tool	*Cost Function*		*Improvement Percentage*
	Φ_0^{fine}	Φ_{SbD}^{fine}	
Full	663.46	661.78	-0.25%
Truncated	663.51	661.75	-0.26%

Table 4: Cost Function Improvement.

1.1.3 Test Case #3 - Single Frequency - 1 Anisotropic WAIM Layer - $\varepsilon^1 = [1 : 35] + j0$ - Square Lattice - $\varepsilon^{sub} = 12.8$ Tests

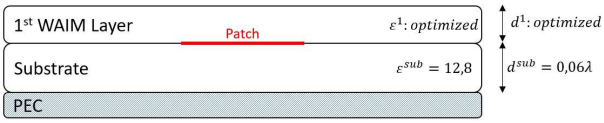

Figure 9: Test Case Schema.

Simulation Parameters:

- Frequency: $f = 10[GHz]$;
- Patch dimensions: $w = 0.15$, $l = 0.098$ $[\lambda]$;
- Probe position: $x = 0.049$, $y = 0.0$ $[\lambda]$;
- Substrate: $\varepsilon_x = 12.8 + j0$, $\varepsilon_y = 12.8 + j0$, $\varepsilon_z = 12.8 + j0$, $d = 0.06[\lambda]$
- Floquet coefficient = 121;
- Lattice basis: $s_1 = (0.5, 0.0)$, $s_2 = (0.0, 0.5)$ $[\lambda]$;

Analysis Parameters:

- Samples analysis (phi cuts): $\theta \in [0, 90]$ $[deg]$, $\varphi \in [0, 90]$ $[deg]$, $\theta_{samples} = 182$, $\varphi_{samples} = 3$;
- Samples analysis (3D plots): $\theta \in [-180, 180]$ $[deg]$, $\varphi \in [-90, 90]$ $[deg]$, $\theta_{samples} = 72$, $\varphi_{samples} = 21$;

PSO Synthesis Parameters:

- Number of WAIM Layers: $N = 1$;
- Unknowns: $U = 4$;
- Unknown ranges: $\varepsilon_{xx} = [1 : 35] + j0$, $\varepsilon_{yy} = [1 : 35] + j0$, $\varepsilon_{zz} = [1 : 35] + j0$, $d = [0.033 : 0.5]$ $[\lambda]$;
- Swarm size: $P = 6$;
- Max iteration number: $I = 80$;
- Inertial weight= 0.4;
- Alpha= 0.4;
- Beta= 0.4;
- C1= 2.0;
- C2= 2.0;

- Random seed= 26;
- No-WAIM case implemented by the first particle at the 1^{st} iteration;
- Samples synthesis (phi cuts): $\theta \in [0,\ 90]\ [deg]$, $\varphi \in [0,\ 90]\ [deg]$, $\theta_{samples} = 7$, $\varphi_{samples} = 3$;

Optimization Results

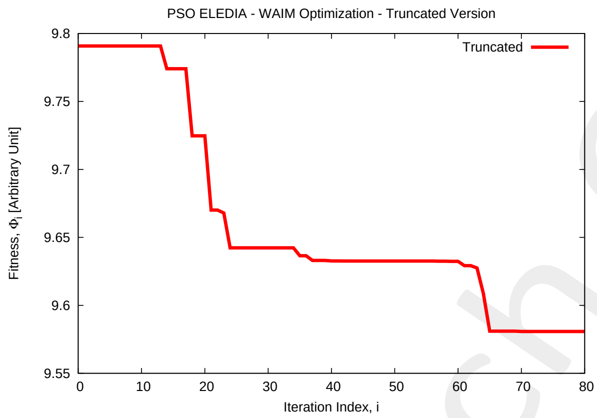

Figure 10: Fitness Dynamics.

$$Simulation\,time\,(Truncated):\ 298m\,51s$$

From the previous tests, we have seen that dealing with Isotropic materials does not lead the big improvements in the radiation performance of the array. Indeed, even if we set ranges of ε^1 with an high maximum value, the optimal solution will tend to Free Space values. Thus, in this simulation, we will consider Anisotropic materials. All the ε components (ε_x^1, ε_y^1 and ε_z^1) have the same range ($[1\ :\ 35] + j0$), but their value will be optimized singularly, as independent variables.

Tool	*Optimal Solution*				*Fitness Value*	
	ε_x^1	ε_y^1	ε_z^1	$h^1\ [\lambda]$	$\Phi_{i=0}$	$\Phi_{I=80}$
Truncated	1.015	8.904	1.376	0.49	9.791	9.581

Table 5: Optimal Solution.

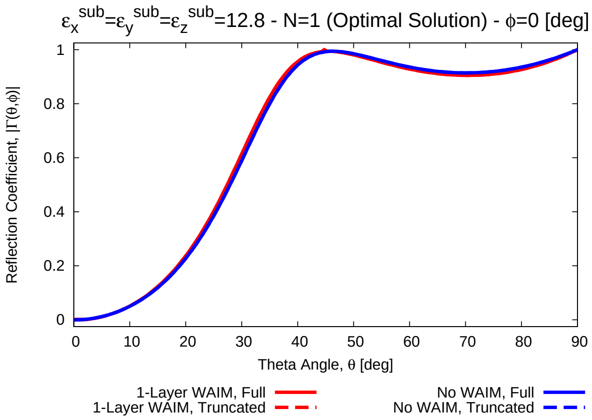

$(a)\ \Gamma,\ \varphi = 0[deg]$

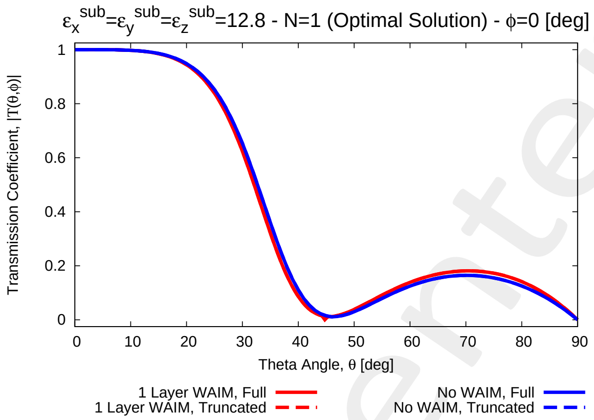

$(b)\ |T|^2,\ \varphi = 0[deg]$

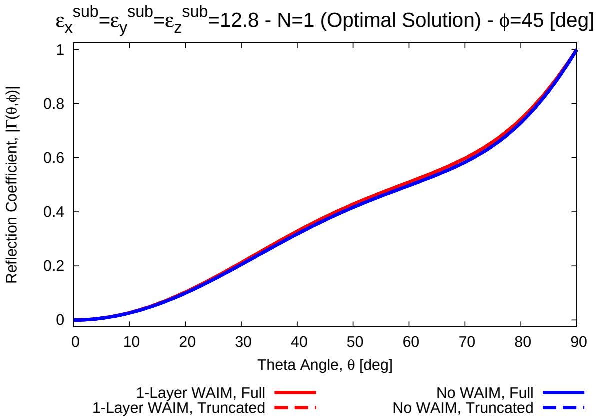

$(c)\ \Gamma,\ \varphi = 45[deg]$

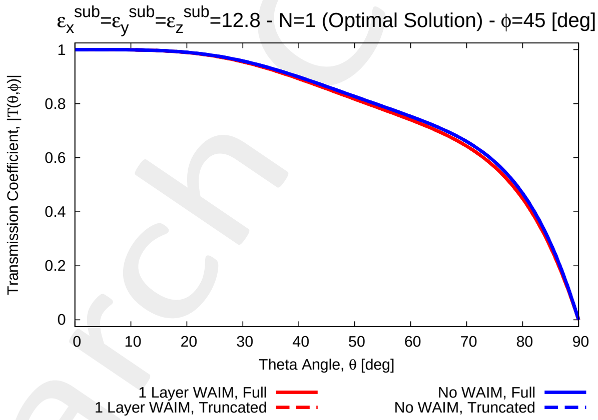

$(d)\ |T|^2,\ \varphi = 45[deg]$

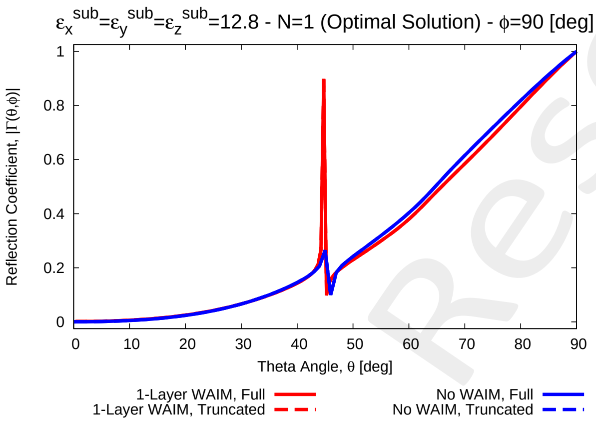

$(e)\ \Gamma,\ \varphi = 90[deg]$

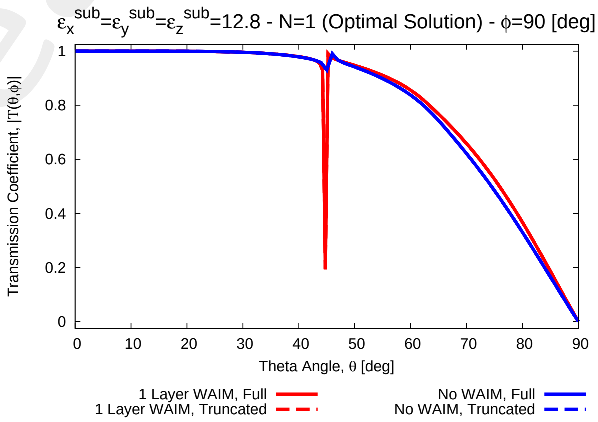

$(f)\ |T|^2,\ \varphi = 90[deg]$

Figure 11: Reflection Coefficient along φ cuts, 1 Layer WAIM.

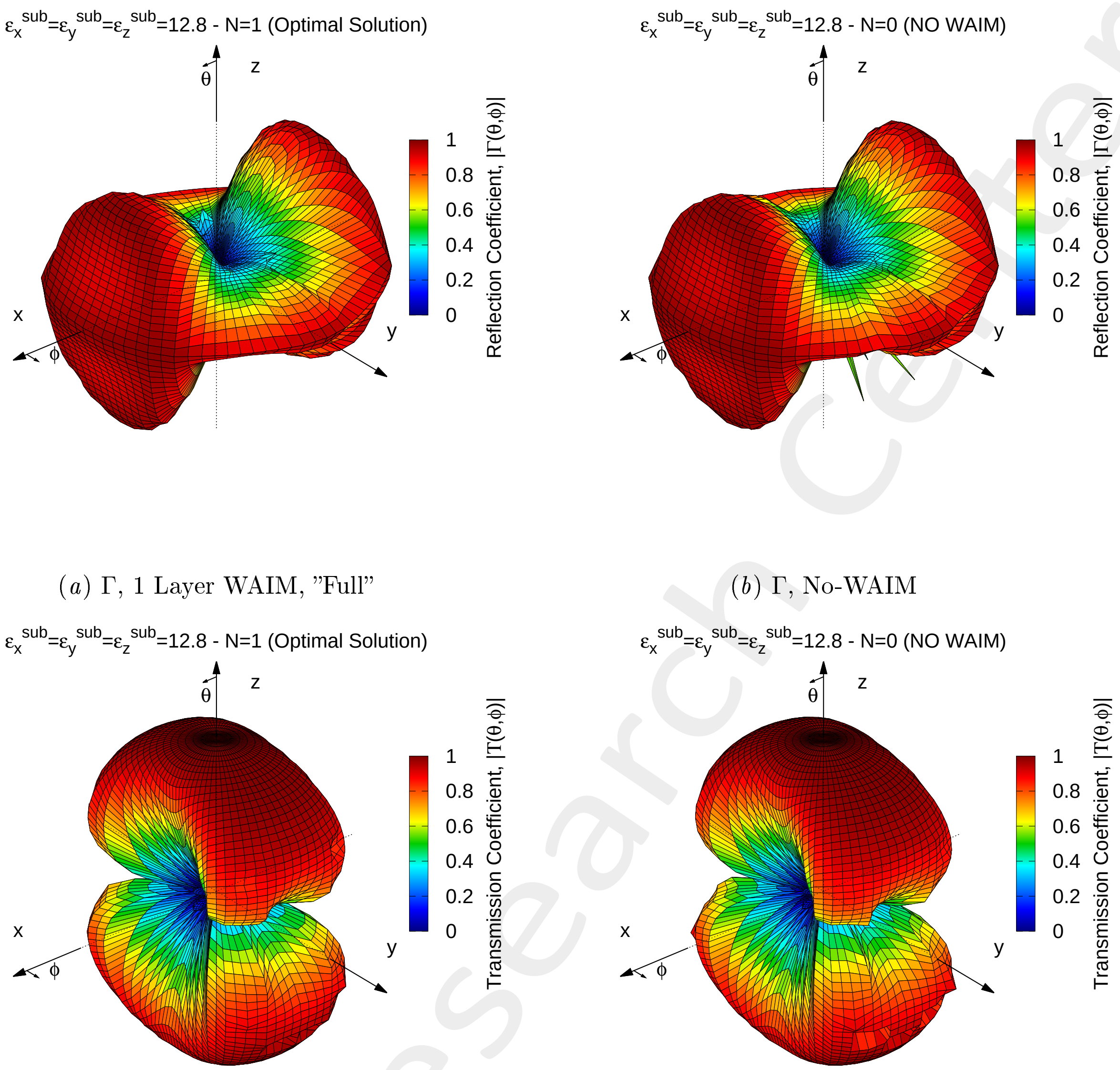

(a) Γ, 1 Layer WAIM, "Full"

(b) Γ, No-WAIM

(c) $|T|^2$, 1 Layer WAIM, "Full"

(d) $|T|^2$, No-WAIM

Figure 12: Reflection Coefficient and Transmission Coefficient

Tool	*Cost Function*		*Improvement Percentage*
	Φ_0^{fine}	Φ_{SbD}^{fine}	
Full	663.46	661.78	-0.25%
Truncated	663.51	661.75	-0.26%

Table 6: Cost Function Improvement.

As we can notice from Table 5 on page 12, the values of ε_x^1, ε_z^1 and d^1 and *Fitness* are almost unchanged with respect to the ones obtained in 1.1.2. Instead, the value of ε_y^1 is pretty high. However, the performance obtained are still similar to the Non-Covered case. Therefore, we could infer that it is not possible to improve the radiation performance only by acting on the real part of ε^1 of a single layer. Moreover, some doubts could arise on the effective utility of an Anisotropic material.

1.1.4 Test Case #4 - Single Frequency - 1 Isotropic WAIM Layer - $\varepsilon^1 = [1 : 35] + j[0 : 35]$ - Square Lattice - $\varepsilon^{sub} = 12.8$ Tests

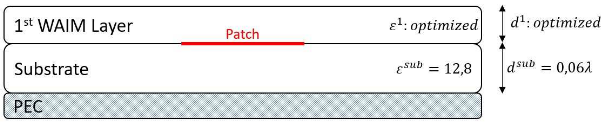

Figure 13: Test Case Schema.

Simulation Parameters:

- Frequency: $f = 10[GHz]$;
- Patch dimensions: $w = 0.15$, $l = 0.098$ $[\lambda]$;
- Probe position: $x = 0.049$, $y = 0.0$ $[\lambda]$;
- Substrate: $\varepsilon_x = 12.8 + j0$, $\varepsilon_y = 12.8 + j0$, $\varepsilon_z = 12.8 + j0$, $d = 0.06[\lambda]$
- Floquet coefficient = 121;
- Lattice basis: $s_1 = (0.5, 0.0)$, $s_2 = (0.0, 0.5)$ $[\lambda]$;

Analysis Parameters:

- Samples analysis (phi cuts): $\theta \in [0, 90]$ $[deg]$, $\varphi \in [0, 90]$ $[deg]$, $\theta_{samples} = 182$, $\varphi_{samples} = 3$;
- Samples analysis (3D plots): $\theta \in [-180, 180]$ $[deg]$, $\varphi \in [-90, 90]$ $[deg]$, $\theta_{samples} = 72$, $\varphi_{samples} = 21$;

PSO Synthesis Parameters:

- Number of WAIM Layers: $N = 1$;
- Unknowns: $U = 3$;
- Unknown ranges: $\varepsilon = [1 : 35] + j[0 : 35]$, $d = [0.033 : 0.5]$ $[\lambda]$;
- Swarm size: $P = 6$;
- Max iteration number: $I = 80$;
- Inertial weight= 0.4;
- Alpha= 0.4;
- Beta= 0.4;
- C1= 2.0;
- C2= 2.0;

- Random seed= 26;
- No-WAIM case implemented by the first particle at the 1^{st} iteration;
- Samples synthesis (phi cuts): $\theta \in [0,\,90]\,[deg]$, $\varphi \in [0,\,90]\,[deg]$, $\theta_{samples} = 7$, $\varphi_{samples} = 3$;

Optimization Results

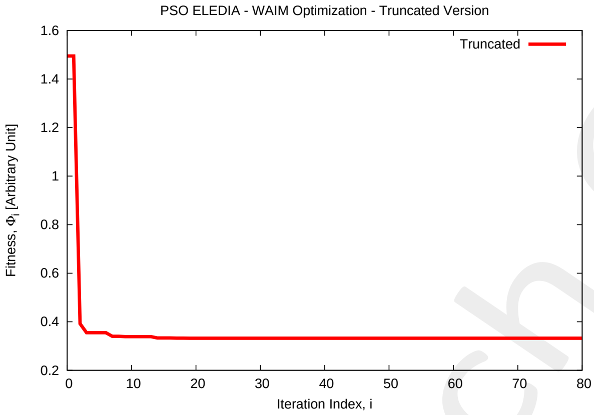

Figure 14: Fitness Dynamics.

$$Simulation\,time\,(Truncated):\;302m\,10s$$

$Tool$	$Optimal\,Solution$			$Fitness\,Value$	
	$Re\{\varepsilon_x^1\} = Re\{\varepsilon_y^1\} = Re\{\varepsilon_z^1\}$	$Im\{\varepsilon_x^1\} = Im\{\varepsilon_y^1\} = Im\{\varepsilon_z^1\}$	$h^1\,[\lambda]$	$\Phi_{i=0}$	$\Phi_{I=80}$
$Truncated$	1.0	5.79	0.23	1.495	0.332

Table 7: Optimal Solution.

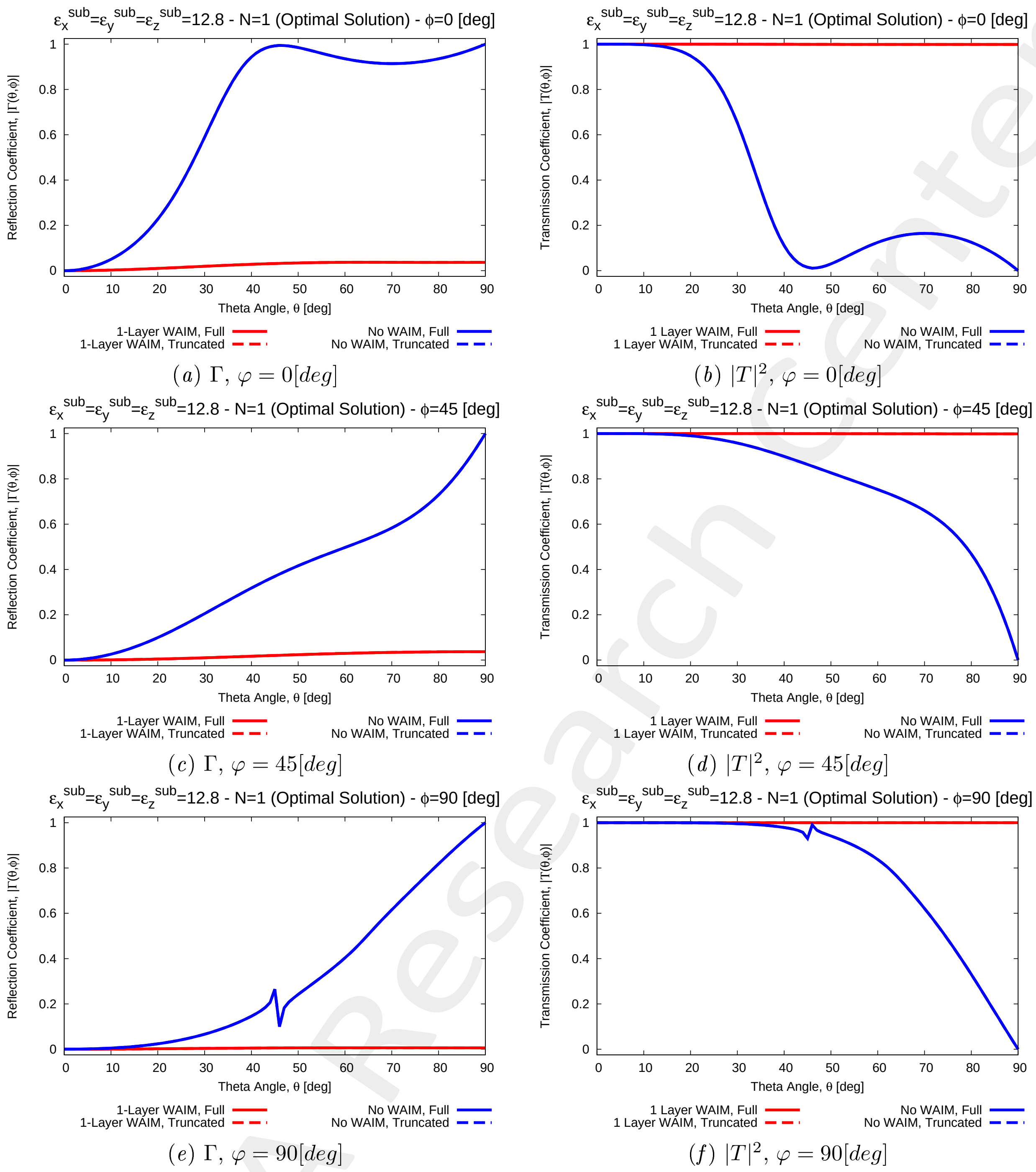

$(a)\ \Gamma,\ \varphi = 0[deg]$

$(b)\ |T|^2,\ \varphi = 0[deg]$

$(c)\ \Gamma,\ \varphi = 45[deg]$

$(d)\ |T|^2,\ \varphi = 45[deg]$

$(e)\ \Gamma,\ \varphi = 90[deg]$

$(f)\ |T|^2,\ \varphi = 90[deg]$

Figure 15: Reflection Coefficient along φ cuts, 1 Layer WAIM.

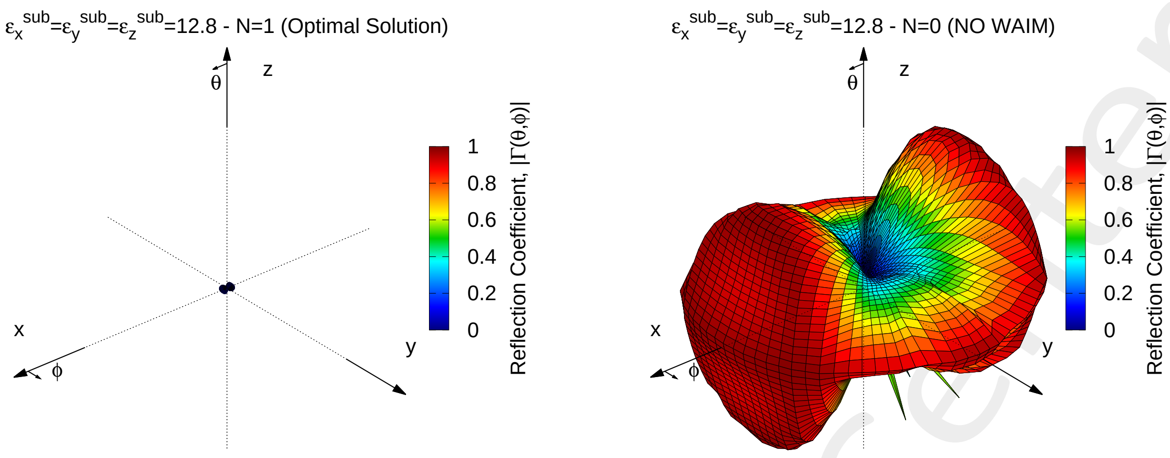

(a) Γ, 1 Layer WAIM, "Full" (b) Γ, No-WAIM

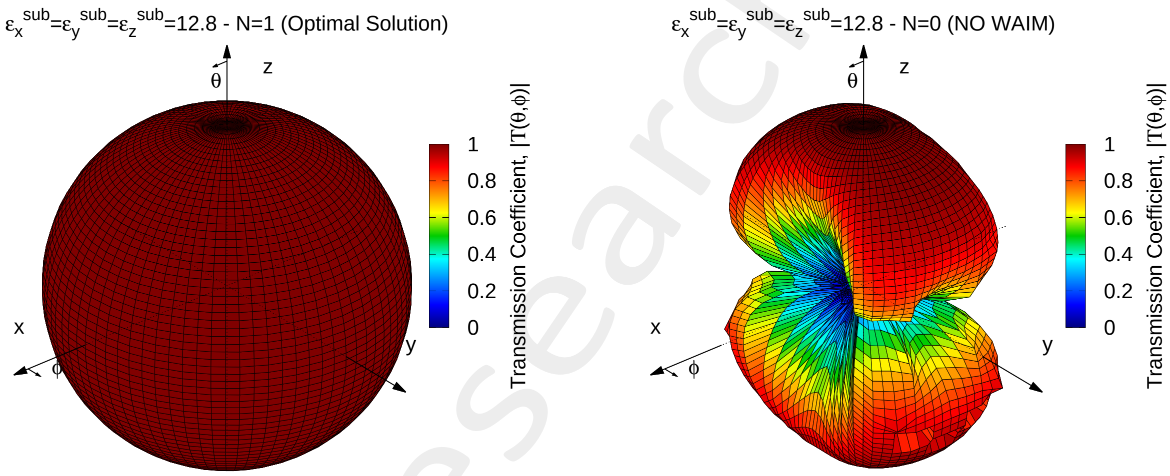

(c) $|T|^2$, 1 Layer WAIM, "Full" (d) $|T|^2$, No-WAIM

Figure 16: Reflection Coefficient and Transmission Coefficient

Tool	*Cost Function*		*Improvement Percentage*
	Φ_0^{fine}	Φ_{SbD}^{fine}	
Full	663.46	23.24	-96.50%
Truncated	663.51	23.33	-96.48%

Table 8: Cost Function Improvement.

Acting on the $Im\{\varepsilon^1\}$, finally, we are able to almost perfectly match the impedance, leading to a an excellent radiation pattern along all the possible steering directions (θ, ϕ).

More information on the topics of this document can be found in the following list of references.

References

[1] P. Rocca, M. Benedetti, M. Donelli, D. Franceschini, and A. Massa, "Evolutionary optimization as applied to inverse problems," Inverse Problems - 25 th Year Special Issue of Inverse Problems, Invited Topical Review, vol. 25, pp. 1-41, Dec. 2009.

[2] P. Rocca, G. Oliveri, and A. Massa, "Differential Evolution as applied to electromagnetics," IEEE Antennas Propag. Mag., vol. 53, no. 1, pp. 38-49, Feb. 2011.

[3] P. Rocca, N. Anselmi, A. Polo, and A. Massa, "An irregular two-sizes square tiling method for the design of isophoric phased arrays," IEEE Trans. Antennas Propag., vol. 68, no. 6, pp. 4437-4449, Jun. 2020.

[4] P. Rocca, N. Anselmi, A. Polo, and A. Massa, "Modular design of hexagonal phased arrays through diamond tiles," IEEE Trans. Antennas Propag., vol.68, no. 5, pp. 3598-3612, May 2020.

[5] N. Anselmi, L. Poli, P. Rocca, and A. Massa, "Design of simplified array layouts for preliminary experimental testing and validation of large AESAs," IEEE Trans. Antennas Propag., vol. 66, no. 12, pp. 6906-6920, Dec. 2018.

[6] N. Anselmi, P. Rocca, M. Salucci, and A. Massa, "Contiguous phase-clustering in multibeam-on-receive scanning arrays" IEEE Trans. Antennas Propag., vol. 66, no. 11, pp. 5879-5891, Nov. 2018.

[7] G. Oliveri, G. Gottardi, F. Robol, A. Polo, L. Poli, M. Salucci, M. Chuan, C. Massagrande, P. Vinetti, M. Mattivi, R. Lombardi, and A. Massa, "Co-design of unconventional array architectures and antenna elements for 5G base station," IEEE Trans. Antennas Propag., vol. 65, no. 12, pp. 6752-6767, Dec. 2017.

[8] N. Anselmi, P. Rocca, M. Salucci, and A. Massa, "Irregular phased array tiling by means of analytic schemata-driven optimization," IEEE Trans. Antennas Propag., vol. 65, no. 9, pp. 4495-4510, September 2017.

[9] N. Anselmi, P. Rocca, M. Salucci, and A. Massa, "Optimization of excitation tolerances for robust beamforming in linear arrays" IET Microwaves, Antennas & Propagation, vol. 10, no. 2, pp. 208-214, 2016.

[10] P. Rocca, R. J. Mailloux, and G. Toso, "GA-Based optimization of irregular sub-array layouts for wideband phased arrays desig," IEEE Antennas and Wireless Propag. Lett., vol. 14, pp. 131-134, 2015.

[11] P. Rocca, M. Donelli, G. Oliveri, F. Viani, and A. Massa, "Reconfigurable sum-difference pattern by means of parasitic elements for forward-looking monopulse radar," IET Radar, Sonar & Navigation, vol 7, no. 7, pp. 747-754, 2013.

[12] P. Rocca, L. Manica, and A. Massa, "Ant colony based hybrid approach for optimal compromise sum-difference patterns synthesis," Microwave Opt. Technol. Lett., vol. 52, no. 1, pp. 128-132, Jan. 2010.

[13] P. Rocca, L. Manica, and A. Massa, "An improved excitation matching method based on an ant colony optimization for suboptimal-free clustering in sum-difference compromise synthesis," IEEE Trans. Antennas Propag., vol. 57, no. 8, pp. 2297-2306, Aug. 2009.

[14] P. Rocca, L. Manica, and A. Massa, "Hybrid approach for sub-arrayed monopulse antenna synthesis," Electronics Letters, vol. 44, no. 2, pp. 75-76, Jan. 2008.

[15] P. Rocca, L. Manica, F. Stringari, and A. Massa, "Ant colony optimization for tree-searching based synthesis of monopulse array antenna," Electronics Letters, vol. 44, no. 13, pp. 783-785, Jun. 19, 2008.

[16] G. Oliveri, A. Gelmini, A. Polo, N. Anselmi, and A. Massa, "System-by-design multi-scale synthesis of task-oriented reflectarrays," IEEE Trans. Antennas Propag., vol. 68, no. 4, pp. 2867-2882, Apr. 2020.

[17] M. Salucci, F. Robol, N. Anselmi, M. A. Hannan, P. Rocca, G. Oliveri, M. Donelli, and A. Massa, "S-Band spline-shaped aperture-stacked patch antenna for air traffic control applications," IEEE Tran. Antennas Propag., vol. 66, no. 8, pp. 4292-4297, Aug. 2018.

[18] M. Salucci, L. Poli, A. F. Morabito, and P. Rocca, "Adaptive nulling through subarray switching in planar antenna arrays," Journal of Electromagnetic Waves and Applications, vol. 30, no. 3, pp. 404-414, February 2016

[19] T. Moriyama, L. Poli, and P. Rocca, "Adaptive nulling in thinned planar arrays through genetic algorithms" IEICE Electronics Express, vol. 11, no. 21, pp. 1-9, Sep. 2014.

[20] L. Poli, P. Rocca, M. Salucci, and A. Massa, "Reconfigurable thinning for the adaptive control of linear arrays," IEEE Trans. Antennas Propag., vol. 61, no. 10, pp. 5068-5077, Oct. 2013.

[21] P. Rocca, L. Poli, G. Oliveri, and A. Massa, "Adaptive nulling in time-varying scenarios through time-modulated linear arrays," IEEE Antennas Wireless Propag. Lett., vol. 11, pp. 101-104, 2012.

[22] M. Benedetti, G. Oliveri, P. Rocca, and A. Massa, "A fully-adaptive smart antenna prototype: ideal model and experimental validation in complex interference scenarios," Progress in Electromagnetic Research, PIER 96, pp. 173-191, 2009.

[23] M. Benedetti, R. Azaro, and A. Massa, "Memory enhanced PSO-based optimization approach for smart antennas control in complex interference scenarios," IEEE Trans. Antennas Propag., vol. 56, no. 7, pp. 1939-1947, Jul. 2008.

[24] M. Benedetti, R. Azaro, and A. Massa, "Experimental validation of a fully-adaptive smart antenna prototype," Electronics Letters, vol. 44, no. 11, pp. 661-662, May 2008.

[25] R. Azaro, L. Ioriatti, M. Martinelli, M. Benedetti, and A. Massa, "An experimental realization of a fully-adaptive smart antenna," Microwave Opt. Technol. Lett., vol. 50, no. 6, pp. 1715-1716, Jun. 2008.

[26] M. Benedetti, R. Azaro, D. Franceschini, and A. Massa, "PSO-based real-time control of planar uniform circular arrays," IEEE Antennas Wireless Propag. Lett., vol. 5, pp. 545-548, 2006.

[27] G. Oliveri, P. Rocca, M. Salucci, and A. Massa, "Holographic smart EM skins for advanced beam power shaping in next generation wireless environments," IEEE J. Multiscale Multiphysics Comput. Tech., vol. 6, pp. 171-182, Oct. 2021.

[28] M. Salucci, L. Tenuti, G. Gottardi, A. Hannan, and A. Massa, "System-by-design method for efficient linear array miniaturisation through low-complexity isotropic lenses" Electronic Letters, vol. 55, no. 8, pp. 433-434, May 2019.

[29] M. Salucci, N. Anselmi, S. Goudos, and A. Massa, "Fast design of multiband fractal antennas through a system-by-design approach for NB-IoT applications" EURASIP J. Wirel. Commun. Netw., vol. 2019, no. 1, pp. 68-83, Mar. 2019.

[30] M. Salucci, G. Oliveri, N. Anselmi, and A. Massa, "Material-by-design synthesis of conformal miniaturized linear phased arrays," IEEE Access, vol. 6, pp. 26367-26382, 2018.

[31] M. Salucci, G. Oliveri, N. Anselmi, G. Gottardi, and A. Massa, "Performance enhancement of linear active electronically-scanned arrays by means of MbD-synthesized metalenses," Journal of Electromagnetic Waves and Applications, vol. 32, no. 8, pp. 927-955, 2018.

[32] G. Oliveri, M. Salucci, N. Anselmi and A. Massa, "Multiscale System-by-Design synthesis of printed WAIMs for waveguide array enhancement," IEEE J. Multiscale Multiphysics Computat. Techn., vol. 2, pp. 84-96, 2017.

[33] A. Massa and G. Oliveri, "Metamaterial-by-Design: Theory, methods, and applications to communications and sensing - Editorial," EPJ Applied Metamaterials, vol. 3, no. E1, pp. 1-3, 2016.

[34] G. Oliveri, F. Viani, N. Anselmi, and A. Massa, "Synthesis of multi-layer WAIM coatings for planar phased arrays within the system-by-design framework," IEEE Trans. Antennas Propag., vol. 63, no. 6, pp. 2482-2496, June 2015.

[35] G. Oliveri, L. Tenuti, E. Bekele, M. Carlin, and A. Massa, "An SbD-QCTO approach to the synthesis of isotropic metamaterial lenses" IEEE Antennas Wireless Propag. Lett., vol. 13, pp. 1783-1786, 2014.

[36] A. Massa, G. Oliveri, P. Rocca, and F. Viani, "System-by-Design: a new paradigm for handling design complexity," 8th European Conference on Antennas Propag. (EuCAP 2014), The Hague, The Netherlands, pp. 1180-1183, Apr. 6-11, 2014.

[37] P. Rocca, G. Oliveri, R. J. Mailloux, and A. Massa, "Unconventional phased array architectures and design Methodologies - A review," Proceedings of the IEEE, vol. 104, no. 3, pp. 544-560, March 2016.

[38] A. Massa, A. Benoni, P. Da RÃ¹, S. K. Goudos, B. Li, G. Oliveri, A. Polo, P. Rocca, and M. Salucci, "Designing smart electromagnetic environments for next-generation wireless communications," Telecom, Invited Paper, vol. 2, pp. 213â221, 2021.

[39] G. Oliveri, D. H. Werner, and A. Massa, "Reconfigurable electromagnetics through metamaterials - A review" Proc. IEEE, vol. 103, no. 7, pp. 1034-1056, Jul. 2015.

[40] I. Martinez, A. H. Panaretos, D. H. Werner, G. Oliveri, and A. Massa, "Ultra-thin reconfigurable electromagnetic metasurface absorbers," EuCAP 2013, Gothenburg, Sweden, Apr. 8-12, 2013.